Evaporative Cooling Due to a Sparse Spray

M. di Marzo & S. Tinker

Mechanical Engineering Department
University of Maryland
College Park, MD 20742

ABSTRACT

The cooling effect of a sparse spray impinging on a semi-infinity solid is investigated. Experiments are conducted by monitoring, via infrared thermography, the surface of the solid heated by radiation and cooled by sprays of uniform size droplets until steady state conditions are reached. The surface temperature field in the proximity of a single droplet is modeled with a closed-form solution based on the hypothesis of constant and uniform heat flux at the solid-liquid interface. In the far-field, an instantaneous point-sink solution is adequate to represent a single droplet cooling effect. These closed-form solutions are used to fit the results of a coupled model, previously developed, which solves the liquid and solid temperature field for the evaporative transient. Inputs from this model are necessary for the formulation of both the closed-form solutions. The spray model formulation is based on the superposition of the cooling effect of all the droplet deposited on the surface. The transient surface temperature distributions and the average surface temperature are compared for the data and computations. The results are in good agreement for similar random droplet distributions of the order of one g/m^{2}s with initial solid surface temperatures ranging between 130 and 160 °C.

NOTATION

c	specific heat of the solid
D	cumulative droplet distribution in the region bounded by r^*
erf	error function
J_0, J_1	Bessel's functions
k	thermal conductivity of the solid
r	generic radial coordinate
r^*	normalized radius of the spray: see Eq. (1)
R	radius of the wetted region under an evaporating droplet
q_c	average heat flux at the solid-liquid interface
q_0	steady state heat flux in the solid prior to the spray activation
T	solid surface temperature
T_0	solid surface temperature prior to the spray application
α	thermal diffusivity of the solid
β	droplet shape parameter after deposition
θ	contact angle receding value
λ	dummy variable of integration
ρ	density of the solid
τ	droplet evaporation time

INTRODUCTION

Spray cooling finds application in quenching processes, in surface coating, in cooling towers and in a number of other industrial processes. The large heat removal associated with the water vaporization is the key characteristic of spray cooling. Several researchers have studied the fundamental mechanism of single droplet and multi-droplets evaporation. Early investigations by Toda [1] and Bonacina [2] provide the fundamental insight in the performance of water sprays and mists. Models of the cooling effect of sprays are proposed by Tio and Sadhal [3] and Rizza [4].

In the specific area of fire protection, sprinkler and mist technologies are based on spray cooling. The sprinklers are designed to effectively extinguish a developing fire and typically involve significant water fluxes. With the elimination of alogenated agents, due to environmental concerns, a more sophisticated usage of light water sprays and mists may find application in the protection of valuable items. Especially in locations exposed to a developing fire, there might be a need to protect items exposed to radiant heat input. In this case, the temperature levels on the solid surfaces are low enough to confine the vaporization processes to evaporative cooling. This implies that the surface temperatures are such that onset of nucleate boiling is not observed. The potential for water damage is higher at these low temperature since the water vaporization rate is reduced.

The motivation for this study is to investigate the behavior of a water spray in these conditions, which require water fluxes of the order of 1 g/m^2s. Note that these water fluxes are about one order of magnitude less than the mist water fluxes required for extinguishment [5]. The droplet size used are one order of magnitude larger than those used in mists applications to insure that the water will reach the solid surface thus protecting it from the fire exposure.

A progression of studies provides the basic understanding to construct a multi droplet model which encompasses: a) the detailed description of the evaporative mechanism and b) a simple representation of each droplet cooling effect. To achieve these objectives, single droplet evaporative transients are investigated with increasingly complex boundary conditions.

At first the droplet is evaporated on a high conductivity material heated from below [6]. In this case, the solid-liquid interfacial condition is almost isothermal and Seki [7] estimates the "contact temperature" from the classical closed-form solution of two infinite solids brought in sudden contact. The study of single droplets deposited on high thermal conductivity materials focusses on the validation of two hypotheses: a) the liquid-vapor boundary condition is dictated by a simultaneous heat and mass transfer, and b) the effect of convective motion in the liquid is negligible. The validity of the second hypothesis is confirmed also by other investigators [8] and allows the treatment of the liquid with a simple heat conduction equation.

Experiments and modeling of evaporation on low thermal conductivity solids provide the description of the solid-liquid boundary [9]. The coupling of the solid and liquid thermal domains is not amenable to finite difference integration due to the sharp temperature gradients in the proximity of the droplet outer edge. The use of boundary element methods circumvents this difficulty. Two major findings results from these studies: a) the realization that the liquid thermal behavior is nearly one-dimensional, in the direction orthogonal to the solid surface, and b) the favorable comparison of the model predictions with those obtained with a closed-form solution based on uniform and constant heat flux under the droplet. Note that the closed-form solution provides an overall temperature distribution on the solid surface which understates the cooling effect under the droplet while exhibiting a slightly broader cooling effect away from the droplet. In the following, the overall effect

of these discrepancies will be outlined the comparison of the spray model prediction with the infrared thermographic data. An additional outcome of these experimental investigations is the development of non-intrusive infrared thermography for the monitoring of the solid surface transient thermal behavior [10]. This measurement technique enables the validation of the model for this case and for all the subsequent more complex situations.

The application of evaporative cooling to fire protection suggests the use of radiant heat input from above rather than the conductive boundary condition previously used. Experimental and theoretical studies are performed in a radiant environment with the same infrared instrumentation [11] and with models which incorporate the effect of the direct radiation as well as the heat input by conduction from the solid [12,13]. These models, validated against a large experimental database, constitute the background information necessary to formulate the multi-droplet model that will be described in the following.

The objective of this paper is to describe: a) the experimental results for the evaporative cooling of a solid subjected to the impingement of a sparse spray and b) the formulation of a model for the prediction of the thermal transients observed experimentally.

EXPERIMENTS

The experimental apparatus is depicted in Fig. 1. The droplet generator is suspended by four cables and is oscillating within a circular region while three bumpers, which move in and out radially at a given frequency, collide randomly with it. Both the shape and the motion frequency of the bumpers are optimized to produce a random motion of the droplet generator. The water droplets, ejected from the generator, have uniform size and impinge upon a Macor tile (square in shape with 15.2 cm sides

and 2.54 cm thickness) mounted below. Macor is a glass-like material with density of 2520 kg/m^3, thermal conductivity of 1.297 W/m °C, specific heat of 888.9 J/kg °C and emissivity of 0.84. The tile lower surface is maintained at a constant temperature of about 30 °C by a chilled plate to provide a controlled thermal boundary condition.

The heat input is provided by three radiant panels. Two of which are mounted symmetrically with respect to the Macor surface at an angle of 30° and the third, lower in aspect ratio, surrounds the Macor tile. The panels are capable of temperatures in excess of 800 °C and they can be approximated to radiate as black-bodies. A 208 V three-phase electric supply is used to power them via a feedback controller which monitors the temperature of the panels heating elements. The position of the panels is important to avoid direct reflection of the incoming radiation to the infrared camera (Inframetrics Model 525). To eliminate additional sources of stray radiation, the camera focusses on the Macor surface through a chilled pipe. The monochrome infrared image is recorded by a high-resolution 8-mm VCR.

The test procedure prescribes a surface cleaning routine and the subsequent exposure of the Macor tile for long period of time (i.e. about two hours) to the radiant heat input. Steady-state conditions are reached and the infrared instrumentation is also brought on-line and stabilized over a long period of time. A reservoir of degassed, deionized water is connected to the droplet generator. A special oil-sealed system is used to prevent gasses (i.e. air) from dissolving in the water. A frequency of droplet deposition is selected and measurements of the water flow rate are obtained to insure the steadiness of the spray dispensing system.

The typical droplet size used in these experiments is of 10 ± 1 μl. The droplet frequency ranges from 0.07 to 0.6 which corresponds to mass fluxes between 0.2 and 1.6 g/m^{2}s over the spray

surface. The droplet distribution is characterized in separate tests using the same equipment. To describe the droplet distribution, a polynomial function is defined which satisfies the following conditions: a) at the center of the spray the droplet distribution is proportional to the surface area; b) at a normalized spray radius of 0.6 the distribution reaches its maximum since for larger radii, the effect of the bumpers is increasingly restricting the droplet generator motion; c) at the outermost radius the generator is nil since it is impossible for the distributer to reach that location due to the presence of the bumpers; d) the distribution is normalized over the spray area. With these conditions the integrated distribution is:

$$D = 1.83\ r^5 - 5.66\ r^4 + 3.83\ r^3 + r^2 \qquad (1)$$

Where the radius is normalized with respect to the spray radius of 0.034 m. This expression fits reasonably well the experimental data as can be seen in Fig. 2.

The correlation between the infrared and temperature scales is obtained by measurements of a black body source in a separate calibration routine. Prior to the activation of the spray, the initial uniform solid surface temperature is detected with a thermocouple probe and this information is used to reference the infrared readings. The details of the calibration procedure are given by Klassen [10]. The infrared thermography is non-intrusive, provides a reasonable temperature resolution and an excellent spatial resolution. The resulting database is extensive since each test lasts for 15 minutes approximately. About 30,000 frames are available for each transient. Each infrared frame can be grabbed and digitized pixel-by pixel yielding about 240,000 independent temperature readings per frame. The uncertainty associated with the temperature readings is of ± 2 °C and the typical spatial resolution is of about 100 μm. The raw data for one frame, where one out of five pixel is sampled,

is presented in Fig. 3. Each square in the figure represents a surface area of 0.40 mm^2. The dark region is bounded by two isothermal lines at 130 °C and 100 °C respectively.

Five initial solid surface temperatures, with several water fluxes, have been investigated for a total of 14 transients. The onset of nucleate boiling for a water droplet deposited on Macor is observed at about 163 °C. The initial solid surface temperatures investigated are: 111, 131, 151, 162 and 182 °C. The water fluxes used are compatible with these temperature levels. This means that lower water fluxes are used with the lower temperatures in order to avoid flooding of the surface.

The results indicates that for several tests at the high water fluxes, the long-term average surface temperature drops well below 100 °C. Therefore, these tests are of limited interest here and will not be considered for the model validation. Note that the spray model cannot be applied to the 182 °C test where nucleate boiling is present. The cooling effect associated with nucleate boiling is completely different from the one modeled here. The spray model will be compared with three sets of data at 131 °C, 151 °C and 162 °C respectively.

MODELING

The modeling of the evaporative transient for a single droplet has been completed and reported in a series of publications [9,12,13]. In particular, a closed-form solution, which describes the transient thermal behavior of a solid surface in the proximity of an evaporative droplet, has been derived as:

$$T_0 - T = \frac{(q_c - q_0)\, R}{k} \int_0^\infty J_0(\lambda r)\, J_1(\lambda R)\, erf(\lambda \sqrt{\alpha t})\, \frac{d\lambda}{\lambda} \tag{2}$$

$$T_0 - T = \frac{(q_c - q_0)\, R}{k}$$

$$\times \int_0^\infty J_0(\lambda r)\, J_1(\lambda R)\, \{erf(\lambda\sqrt{\alpha t}) - erf[\lambda\sqrt{\alpha(t-\tau)}]\}\, \frac{d\lambda}{\lambda} \tag{3}$$

This closed-form solution is obtained applying a constant and uniform condition over a circular portion of the surface of a semi-infinite body. The second equation describes the surface temperature distribution after the heat flux has been removed (i.e. after the complete evaporation of the droplet) as the surface recovers its original state.

This solution has been modified for the case of a water droplet subjected to radiant heat input, while evaporating on a the surface of a solid with low thermal conductivity [13]. The effect of direct radiation on the droplet is to decrease the surface tension and to increase the droplet spreading on the surface [11]. The flatter droplet configuration results in the early decrease of the contact angle to its receding value. Thereafter, the wetted region under the droplet shrinks. A multiplier has been introduced to account for this droplet shrinkage during the later portion of the evaporative transient. A solid-liquid coupled model which uses a boundary element method for the solid domain and a 1-D solution for the liquid, has been developed previously [13]. This model has been described in detailed in previous papers and for the discussion of its features, the reader can consult those references. Note that this model requires two inputs from the experiments: a) the droplet shape parameter, β; b) the receding angle, θ. The droplet shape parameter and the receding angle are obtained experimentally for single droplets deposited over any given solid surface. In general, while sufficiently repeatable, these parameters are strong functions of the surface condition and of the experimental procedures.

Typically, the receding angle is a constant value while the shape parameter may have some minor dependency on the initial solid surface temperature. The coupled model results are reasonably fitted by the closed-form solution if 0.9 R is used instead of R in the term preceding the integral on the right hand side of Eqs. (2) and (3).

Note that, in order to apply the closed-form solution previously described, two parameters must be known: a) the single droplet evaporation time, τ; and b) the portion of the heat flux which contributes to evaporative process by conduction from below the droplet, q_c. The coupled model is used to determine these two parameters. Figure 4 depicts the evaporation time and the conduction heat flux for water droplets of 10 µl deposited on Macor. The closed-form solution obtained in this way approximates reasonably well the coupled model solution up to region under the droplet where discrepancies are observed. This is obvious since the uniform and constant heat flux condition given by the closed-form solution is a poor match for the complex solid-liquid thermal interactions. However, the overall error associated with these discrepancies is very small since the surface involved compared to the overall spray surface is small (less than one percent).

The closed-form solution previously described is used to characterize the surface temperature in the proximity of the droplet. At larger distances ($r > 5$ R, for Macor), a simple, instantaneous point-sink closed-form solution is given as [14]:

$$T_0 - T = \frac{q_c R^2 \tau}{4 \alpha (t - 0.6\tau)^{3/2} \sqrt{\pi \rho c k}} e^{\frac{-r^2}{4\alpha(t-0.6\tau)}} \tag{4}$$

For this solution, the evaporative heat flux contributed by conduction is used. Note that the time of

droplet deposition is augmented by 60 percent of the total evaporation time in order to better approximate the instant when the time-averaged heat removal has occurred. The cut-off between the closed-field and the far-field solution is determined by comparing the two solutions. It is found that for r = 5 R, the maximum difference between the surface temperature computed with the two solutions is of the order of 0.1 °C. Within the uncertainties of the measurements, this would amount to a combined effect of 20 droplets within 5 radii from a given site. Such a droplet density exceed by far the conditions characterized as a sparse spray.

The computational technique for the sparse spray is based on the superposition of the cooling effect of the droplets with respect to the point of concern. This means that each droplet evaporating transient is based on the solid surface temperature at deposition and is not accounting for mutual droplet interactions. This assumption is realistic for the fire protection application which is considered here. In an extinguishment situation, where the droplet density required is higher, this assumption may not apply.

In order to determine the site of deposition for the various droplets, a pairs of random numbers (between 0 and 1) is used to determine each droplet polar position. The first number is used to generate a random azimuthal angle from the center of the spray. The second number is used to generate a radial position for the droplet. The radial position is obtained by solving Eq. (1) while setting the integrated distribution equal to the random number. From Fig. 2 observe that for small values of this number, the droplet is moved to outer positions while for large values of the number the droplet is moved to inner positions. At about 0.6 the number coincides with the actual radial position.

In summary, upon determining the various droplet landing sites and times of deposition, the

superposed effect of all the deposited droplets is evaluated at each point of the computational domain and the temperature of any given point is obtained for any given instant of the transient.

DISCUSSION

The solid surface temperatures within the field of view depicted in Fig. 3 are independently computed with the spray model and the results are shown in Fig. 5 . The computations and the infrared thermography are in reasonable qualitative agreement. There are six droplets on both surfaces at this time and the region bounded by the 130 °C isothermal is slightly smaller in the data plot while the isothermal at 100 °C bounds a larger surface in the same plot the thus yielding an analogous average surface temperature. This is consistent with the slight discrepancies associated with the closed-form solution for the near-field described previously. Note that similar times in the transient have been selected for the data and the model computation. The droplets distribution are independently random and they only match the water flux and droplet distribution but by no mean are identical in droplet deposition sites. The portion of the solid surface considered is identical for the experiment and for the model to insure a similar behavior of the average temperature by considering a similar portion of the spray distribution.

To provide a more quantitative comparison, the average surface temperature is plotted over the duration of the transient for three different tests in Figs. 6 through 8. The oscillatory nature of the temperature is due to the fact that only a portion of the spray area is viewed by the infrared camera. Therefore, at any time, there may be a different number of droplets in the field of view than at other times, resulting in overall variation exhibited in these plots. These comparisons are for tests with initial solid surface temperatures of 131, 151 and 162 °C. They sufficiently demonstrate the

adequacy of the model. Note that for all these plots the transient thermal response of the solid is similar and it exhibits a time constant of about 3 minutes. This result elicits the dominant effect of the substrate heat capacity.

A similar conclusion is derived from considerations of the solid surface temperature behavior for the case with an initial nucleate boiling transient. Figures 9 depicts the average surface temperature during the cooling transient for a test at a low water flux (i.e. 0.50 g/m^2s) with an initial solid surface temperature of 162 °C. For this test, the data up to 3 minutes and for average surface temperatures above 145 °C, exhibit a sharp drop in average surface temperature due to nucleate boiling. Then, upon returning to the evaporative heat transfer regime, the average surface temperature briefly increases (see the arrow in the figure). Thereafter, the temperature resumes its decay at a less steep rate. This phenomenology outlines the significant role played by the stored heat in the solid. Note the marginal upward trend of the data after 7 minutes into the transient. It will take approximately one hour for the steady-state to be reached as the average surface temperature slowly climbs. From these observations it is clear that this set of data is not applicable for model validation since the initial nucleate boiling transient completely changes the thermal behavior of the solid surface.

CONCLUSIONS

A model for the prediction of the cooling effect of a sparse spray applied to a solid surface subjected to radiant heat input is proposed. The model is based on the superposition of the cooling effect of each droplet deposited on the surface. The cooling effect of a single droplet is evaluated by two closed-form solutions for the near and far-field respectively.

The near-field solution assumes uniform and constant heat flux at the solid-liquid boundary

under the evaporating droplet. This closed-form solution is obtained by comparing it with a previously validated coupled-model which describes the vaporization transient. This closed-form solution exhibits slight discrepancies which are reflected in the overall predictions of the spray model. Nonetheless, the overall transient behavior of the solid surface is consistently predicted over a range of conditions.

A few notes concerning the effect of nucleate boiling under the deposited droplet and the realization that the overal time constant is not a strong function of the water flux indicate that the substrate properties play a dominant role on the cooling transient.

ACKNOWLEDGMENTS

This research is sponsored by the Building and Fire Research Laboratory of the National Institute of Standards and Technology (BFRL-NIST). The authors are grateful to Dr. H. Baum (BFRL-NIST) for his guidance in the formulation of the multi-droplet model.

REFERENCES

1. Toda, S., A study of mist cooling. First report: investigation of mist cooling, *Heat Transfer-Jap. Res.* **1** (1972) 39-50.
2. Bonacina,C., Del Giudice, S. & Comini, G., Dropwise evaporation, *Trans. ASME, J. Heat Transfer* **101** (1979) 441-446.
3. Tio, K.K. & Sadhal, S.S., Thermal analysis of droplet spray evaporation from a heated solid surface, *Trans. ASME, J. Heat Transfer* **114** (1992) 220-233.
4. Rizza, J.J., A numerical solution to dropwise evaporation, *Trans. ASMR, J. Heat Transfer* **103**

(1981) 503-507.

5. Milke, J.A., & Gerschefski, C.E., Overview of water mist research for library applications, *ICFRE*, 1995, ed. D.P. Lund - SFPE, pp. 133-138.

6. diMarzo, M. & Evans, D.D., Evaporation of a water droplet deposited on a hot high thermal conductivity surface, *Trans. ASME, J. Heat Transfer* **111** (1989) 210-213.

7. Seki, M., Kawamura, H. & Sanokawa, K., Transient temperature profile of a hot wall due to a impinging liquid droplet, *Trans. ASME, J. Heat Transfer* **100** (1978) 167-169.

8. Ostrach, S. & Pradhan, A., Surface-tension induced convection at reduced gravity, *AIAA J.* **16** (1978) 419-424.

9. diMarzo, M., Tartarini, P., Liao, Y., Evans, D. & Baum, H., Evaporative cooling due to a gently deposited droplet, *Int. J. Heat Mass Transfer* **36** (1993) 4133-4139.

10. Klassen, M., diMarzo, M. & Sirkis, J., Infrared thermography of dropwise evaporative cooling, *Experimental Thermal and Fluid Sci.* **5** (1992) 136-141.

11. diMarzo, M., Kidder, C.H. & Tartarini, P., Infrared thermography of dropwise evaporative cooling of a semi-infinite solid subjected to radiant heat input, *Experimental Heat Transfer* **5** (1992) 101-114.

12. Tartarini, P. & diMarzo, M., Dropwise evaporative cooling in radiative field, *Heat Transfer*, 1994, ed. G.F. Hewitt **6**, pp. 277-282.

13. White, G., Tinker, S. & diMarzo, M., Modelling of dropwise evaporative cooling on a semi-infinite solid subjected to radiant heat input, *Fire Safety Science*, 1994, ed. T. Kashiwagi , pp. 217-228.

14. Carslow, H.S. & Jaeger, J.C., *Conduction of Heat in Solids*, 1959, Oxford Press, pp. 256-258.

CAPTIONS

Figure 1 - Experimental apparatus.

Figure 2 - Integrated droplet distribution: data and curve fit.

Figure 3 - Typical solid surface temperature distribution from the infrared thermographic data: T_o = 151 °C; G = 0.96 g/m^{2}s; t = 300 s (each square represents 0.40 mm^2).

Figure 4 - Evaporation time and conductive heat flux: coupled-model results (x) and curve fits.

Figure 5 - Typical solid surface temperature distribution from the spray model predictions: T_o = 151 C; G = 0.96 g/m ^{2}s; t = 300 s (each square represents 0.40 mm^2).

Figure 6 - Average surface temperature transient: T_o = 131 C; G = 0.50 g/m ^{2}s (the open symbols represent the experimental data and the closed ones represent the spray model computations).

Figure 7 - Average surface temperature transient: T_o = 151 C; G = 0.96 g/m ^{2}s (the open symbols represent the experimental data and the closed ones represent the spray model computations).

Figure 8 - Average surface temperature transient: T_o = 162 C; G = 0.97 g/m ^{2}s (the open symbols represent the experimental data and the closed ones represent the spray model computations).

Figure 9 - Average surface temperature transient: T_o = 162 C; G = 0.50 g/m ^{2}s (the open symbols represent the experimental data and the closed ones represent the spray model computations).

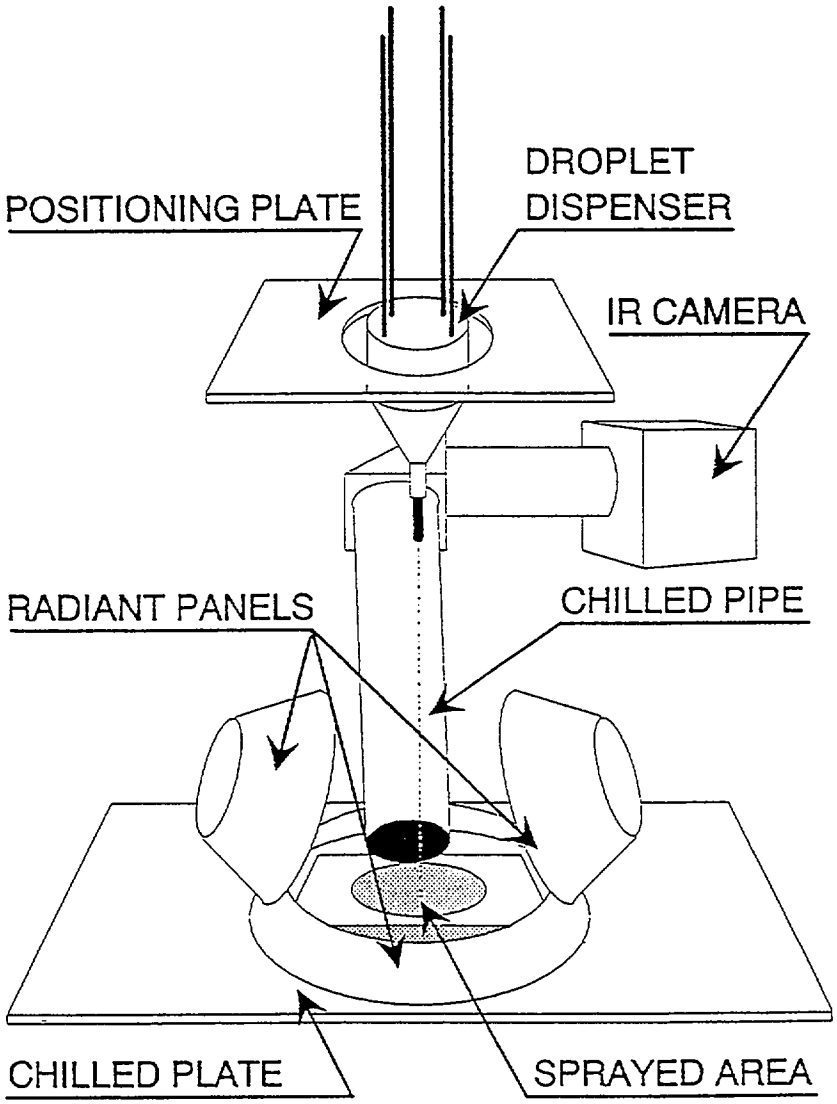
POSITIONING PLATE
DROPLET DISPENSER
IR CAMERA
RADIANT PANELS
CHILLED PIPE
CHILLED PLATE
SPRAYED AREA

FIGURE 1

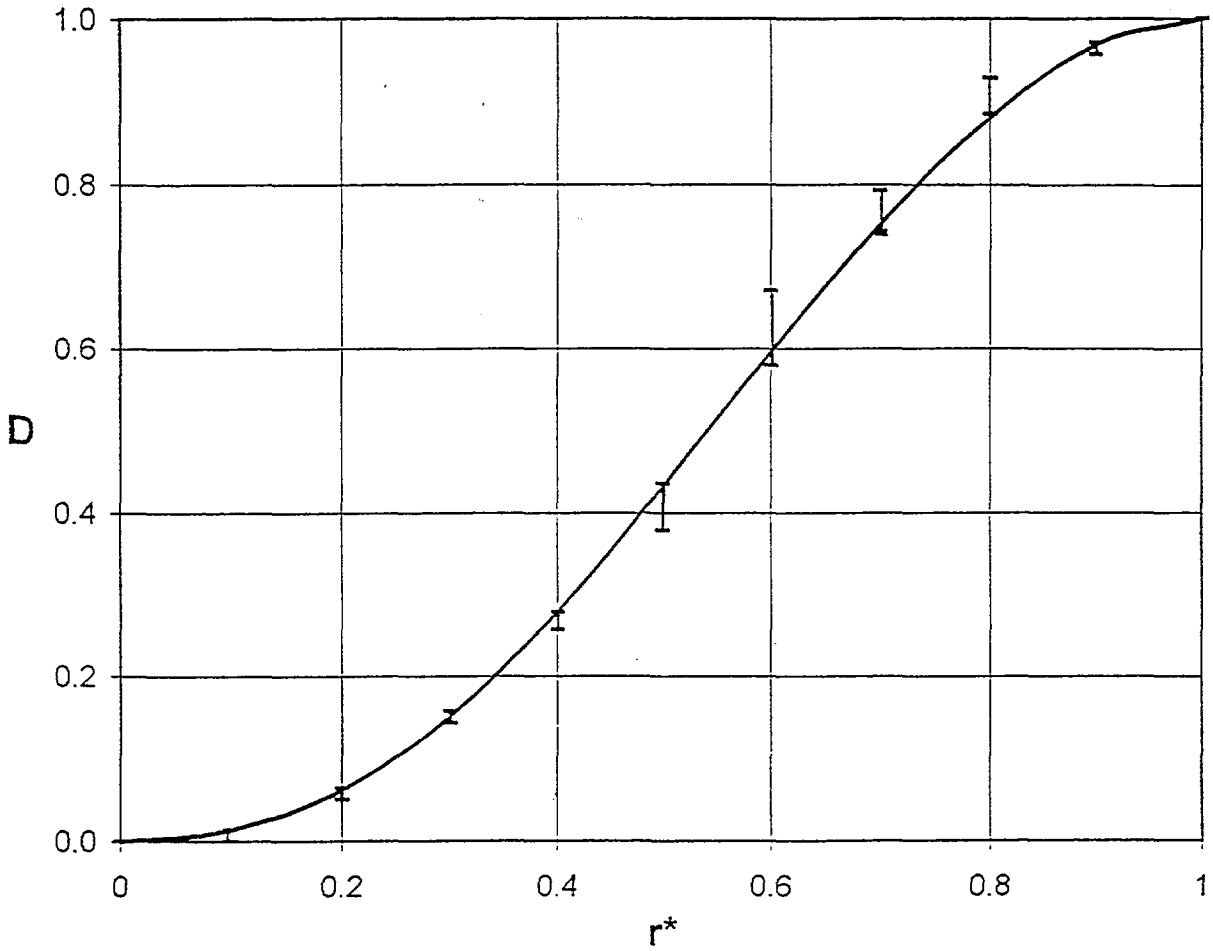

FIGURE 2

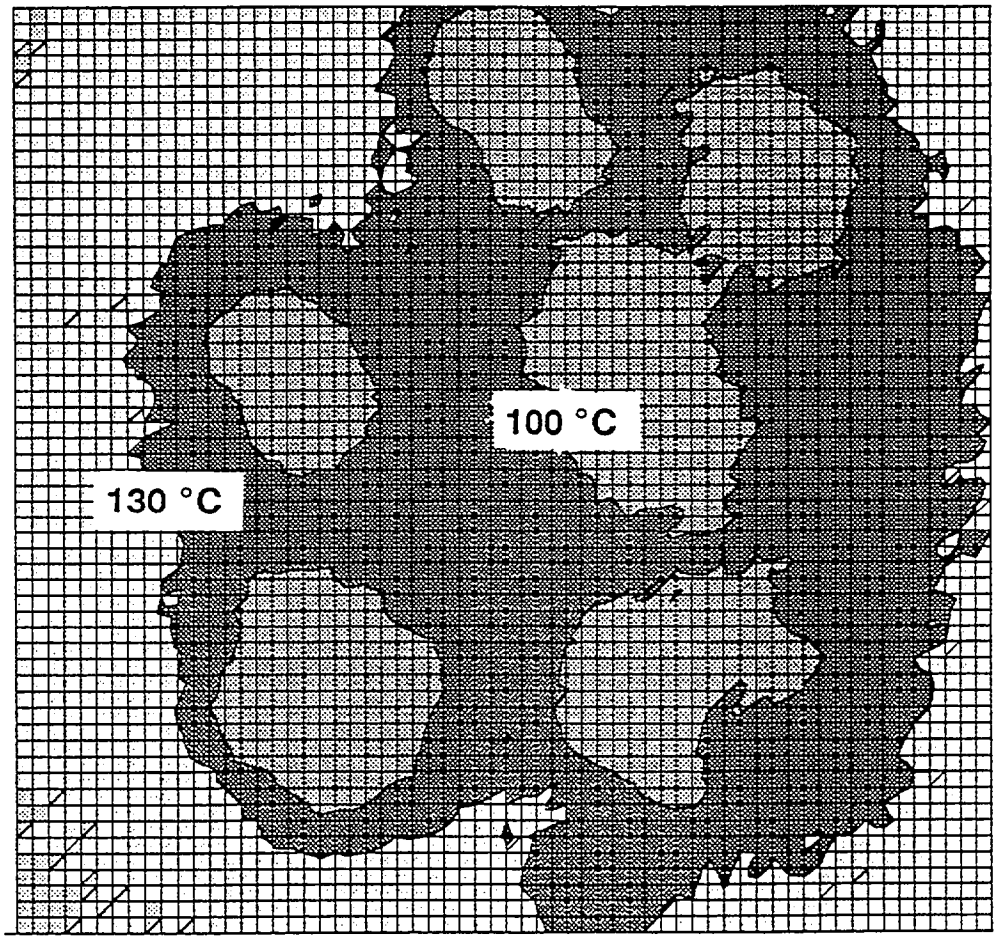

FIGURE 3

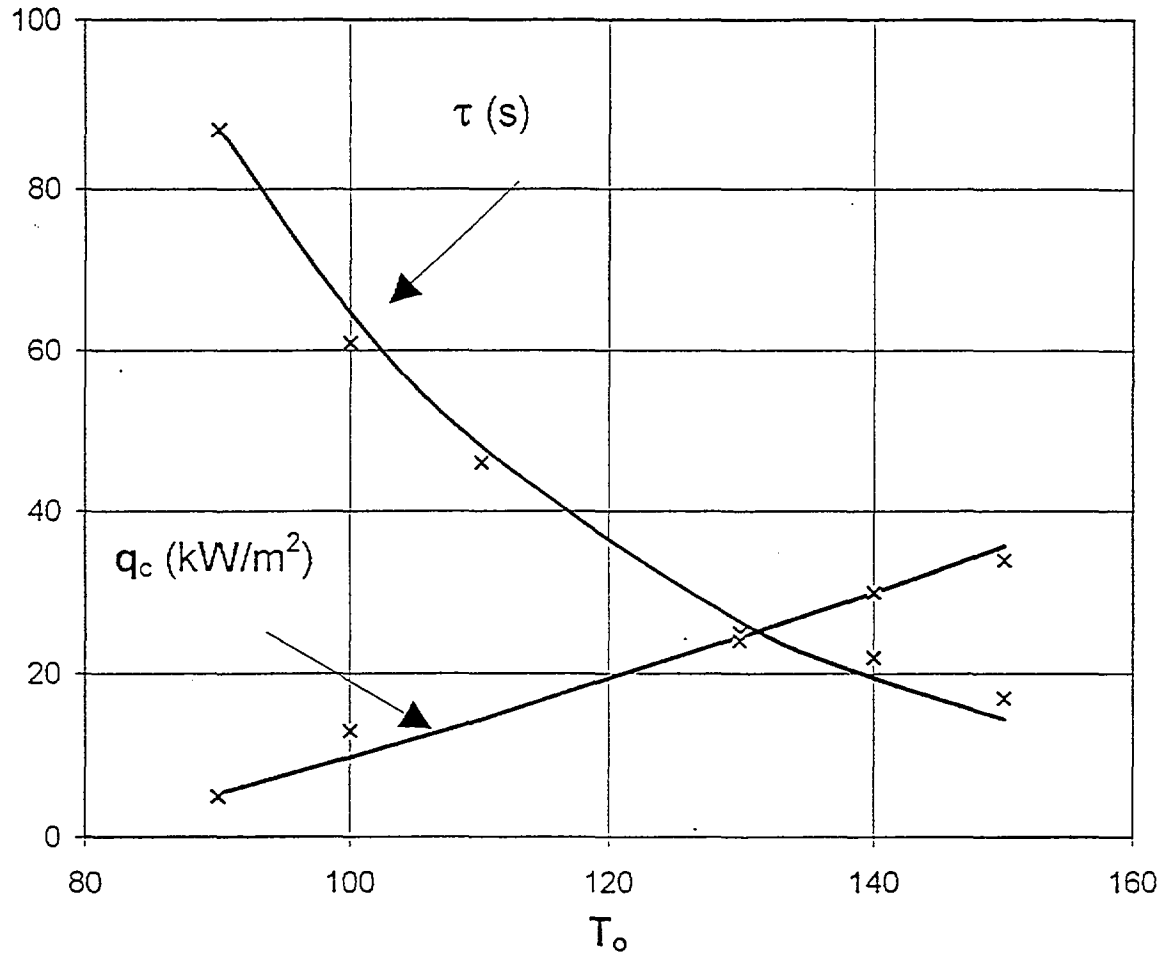

FIGURE 4

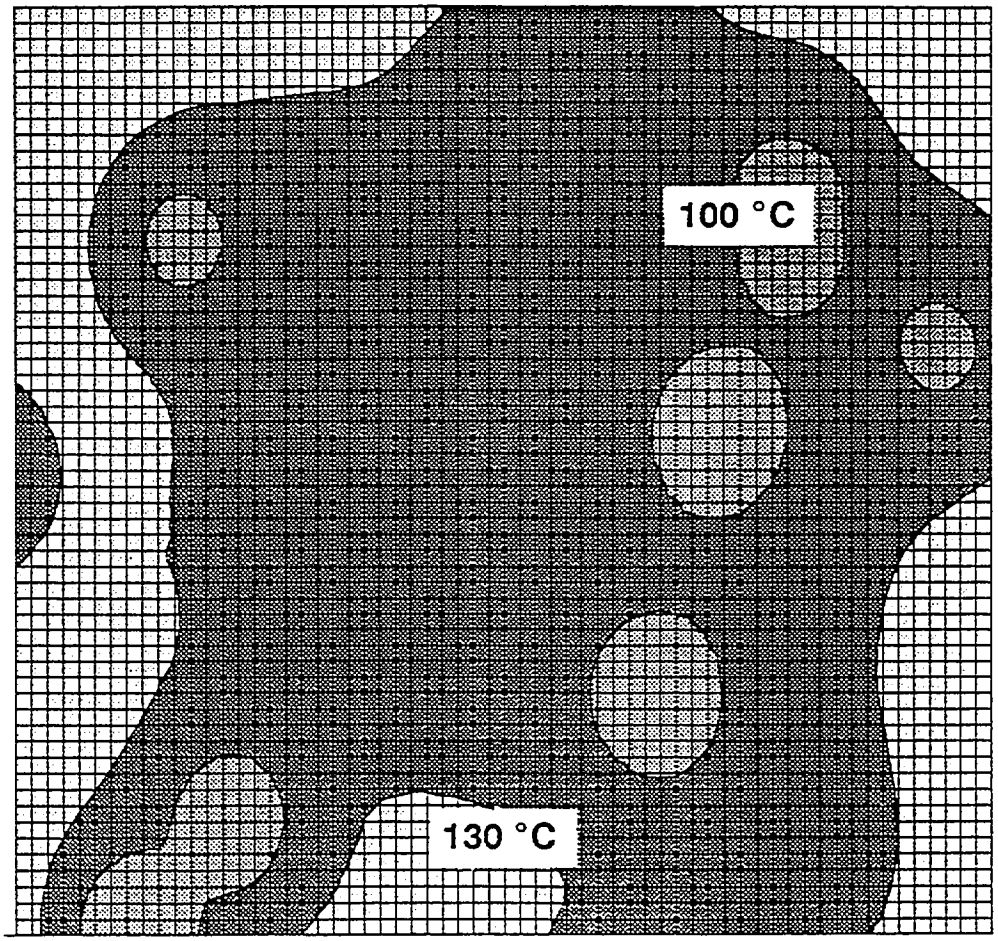

FIGURE 5

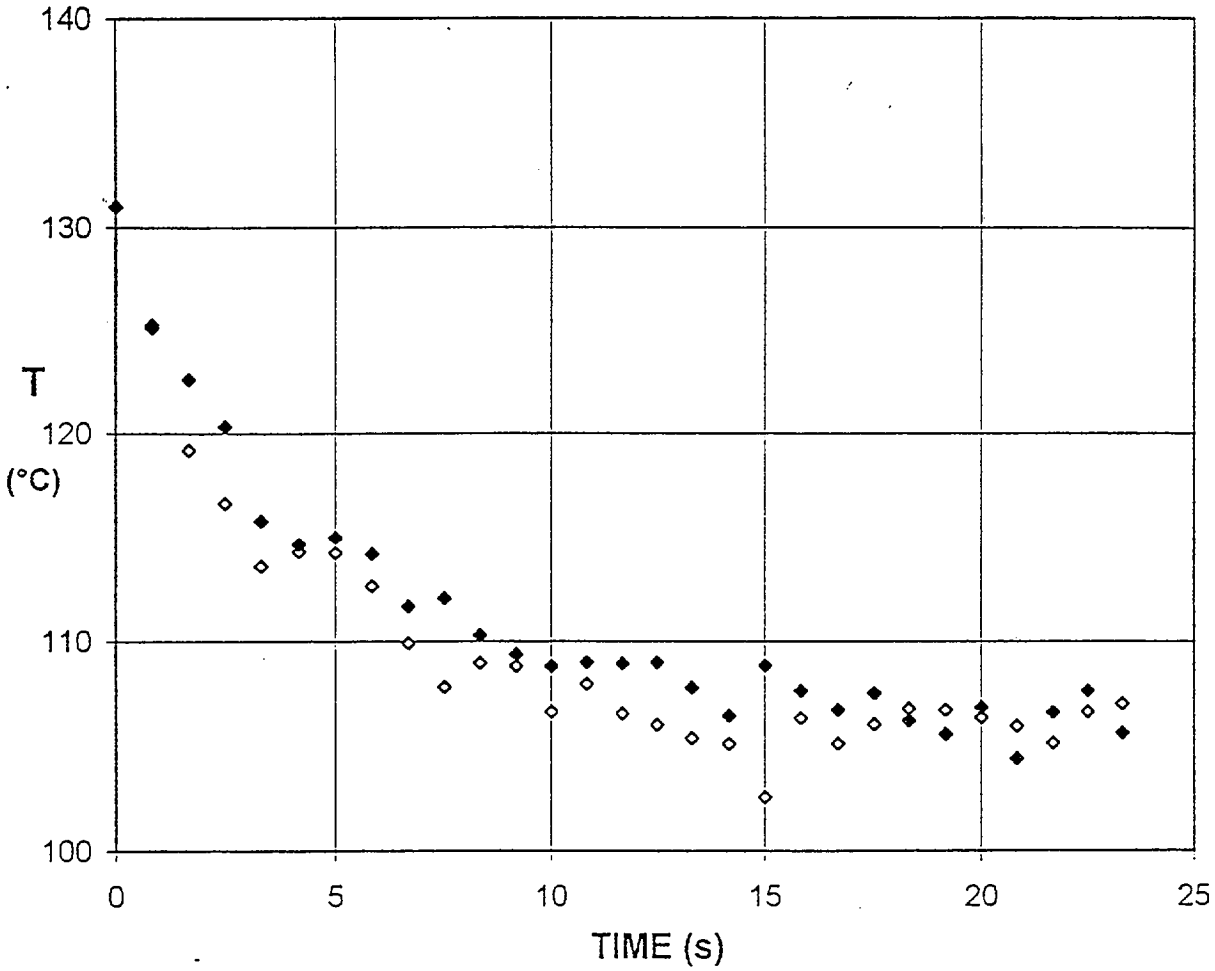

FIGURE 6

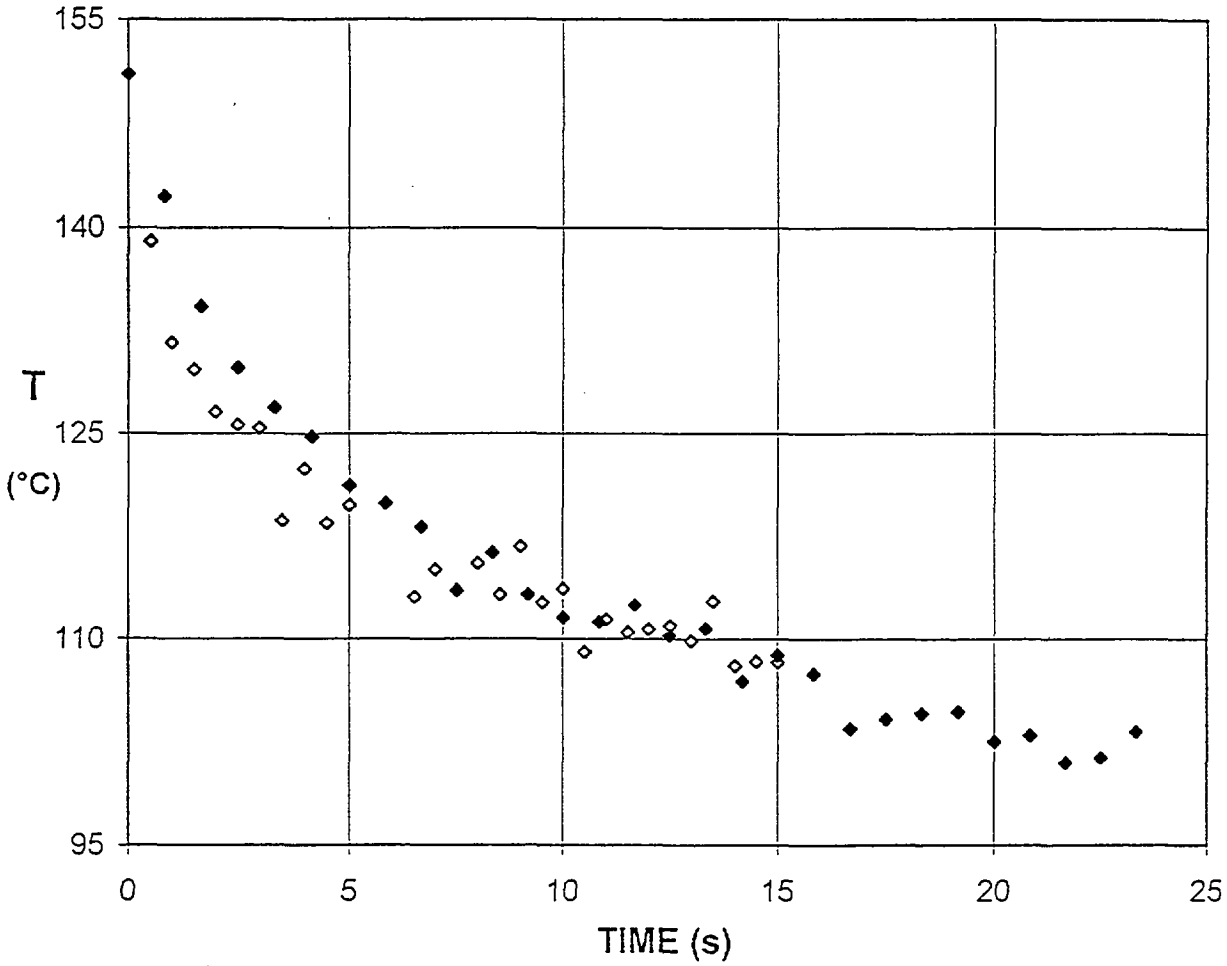

FIGURE 7

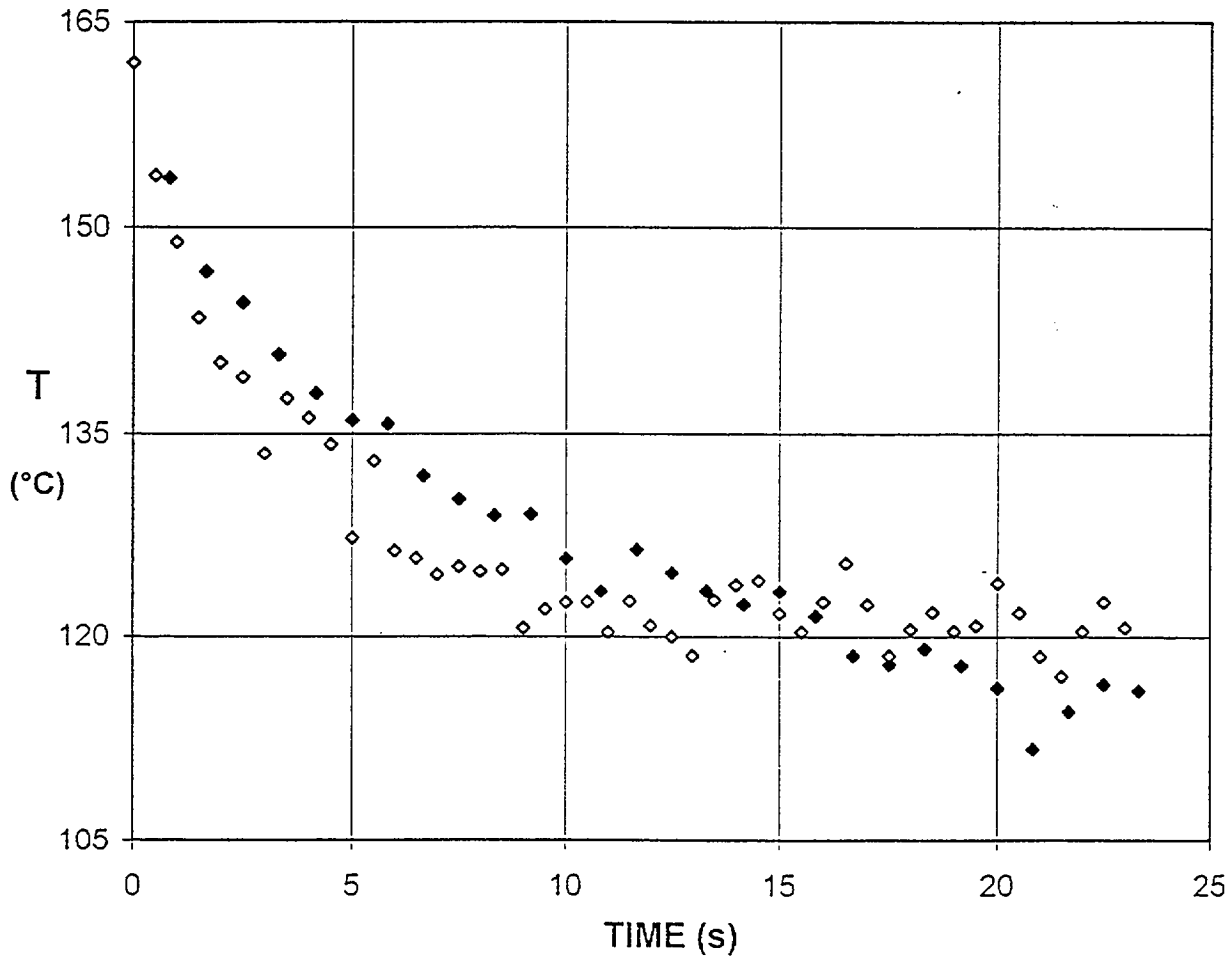

FIGURE 8

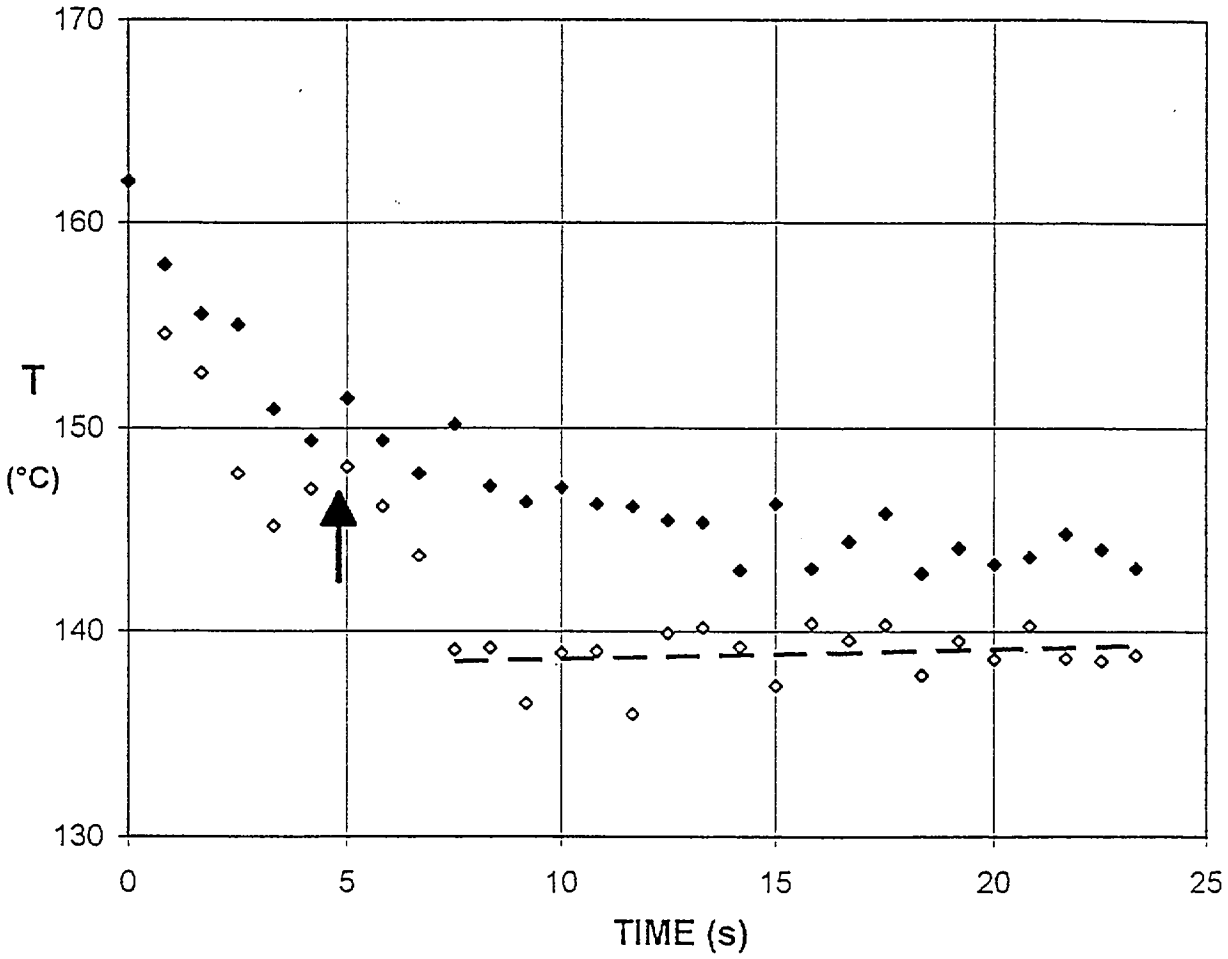

FIGURE 9

APPENDIX A:

Effect of surfactants in the water

S. Chandra, M. diMarzo, Y.M. Qiao & P. Tartarini, Effect of solid-liquid contact angle on droplet evaporation (1995) unpublished manuscript.